Comparative Study of T-amplitude Features for Fitness Monitoring Using the ePatch® ECG Recorder

Julia Rosemary Thorpe[1], Trine Saida[2], Jesper Mehlsen[3], Anne-Birgitte Mehlsen[4], Henning Langberg[2], Karsten Hoppe[5] and Helge B. D. Sorensen[1]

***Abstract*— This study investigates ECG features, focusing on T-wave amplitude, from a wearable ECG device as a potential method for fitness monitoring in exercise rehabilitation. An automatic T-peak detection algorithm is presented that uses local baseline detection to overcome baseline drift without the need for preprocessing, and offers adequate performance on data recorded in noisy environments. The algorithm is applied to 24 hour data recordings from two subject groups with different physical activity histories. Results indicate that, while mean heart rate (HR) differs most significantly between the groups, T-amplitude features could be useful depending on the disparities in fitness level, and require further investigation on an individual basis.**

I. INTRODUCTION

With increasing prevalence of lifestyle-related diseases, there exists a need for effective and wide reaching treatment and prevention methods [1]. Physical activity interventions that encourage regular exercise and improve physical fitness could meet this need, but face challenges such as high drop-out rates and a lack of outcome measurement. Telehealth solutions that incorporate new portable technologies for remote monitoring could help broaden patient reach without increasing cost compared to traditional rehabilitation programmes [2]. It is therefore of interest to develop a reliable fitness monitoring setup, enabling a means of both programme evaluation and participant feedback that might motivate adherence.

Users and context should be carefully considered in selecting an appropriate approach. To avoid increased burden on healthcare systems, involvement from trained professionals should be minimised. To encourage user acceptance, incorporated technologies should be simple to operate, comfortable and discreet. Features selected as markers for fitness level should favour consistent physical training between measurements over activity during measurements.

A. ECG Features for Fitness Measurement

The ECG signal offers insight into cardiovascular health without relying heavily on subject cooperation. Since physical activity programme participants are frequently enrolled as a result of cardiovascular risk [2], the ECG could potentially fulfil other monitoring roles simultaneously. The T-wave of the ECG represents ventricular repolarisation and its amplitude is related to physical fitness [4]. This could be beneficial if stable, observable changes occur with increased fitness that offer new insight over heart rate (HR) measurements alone.

B. ePatch® ECG Recorder

The ePatch® is a CE-marked, three-lead sternal ECG recording device capable of recording two channels of ECG data continuously for 24 hours. It is well suited to telerehabiltiation due to its discreet size and simple operation that enable use outside of a clinical setting. This allows participants to continue daily life and routine exercise sessions.

Fig. 1. The ePatch® ECG device as worn on the sternum.

II. DATA COLLECTION

A. Subject Groups

Two groups of participants are included in this study: (i) a low fitness group comprising participants previously enrolled in a physical activity intervention due to high risk of lifestyle-related disease, and (ii) a high fitness group comprising healthy, highly active participants.

1) Low fitness group: A subset of 20 participants were recruited from a larger study (50 subjects) investigating long term adherence to physical activity programmes in the Copenhagen region of Denmark. All participants were included one year after completing a physical activity intervention to reduce high risk of lifestyle-related diseases. These subjects are expected to have a relatively low fitness level based on this common background. As this is influenced by how strictly subjects adhered to the prescribed exercises, non-homogeneity in fitness level can of course be expected.

[1]Department of Electrical Engineering, Technical University of Denmark thorpejulia at gmail.com
[2]Department of Public Health, University of Copenhagen
[3]Coordinating Research Centre, Frederiksberg Hospital, Nordre Fasanvej 57, 2000 Frederiksberg, Denmark
[4]Department of Clinical Physiology and Nuclear Medicine, Koege Hospital, Lykkebaekvej 1, 4600 Koege
[5]DELTA Danish Electronics, Light & Acoustics, Venlighedsvej 4, 2970, Hørsholm, Denmark

978-1-4244-7929-0/14/$26.00 ©2014 IEEE

2) High fitness group: Twelve highly active individuals were recruited for this study through fitness clubs and social networks in Copenhagen. Subjects provided self-reported information on weekly training hours. One recording was discarded due to increased fever (from an unrelated infection). An age- and gender- matched selection of eleven participants from the low-fitness group was combined with the high-fitness group, resulting in a total balanced dataset of 22 recordings. A summary of group characteristics is provided in table I.

B. Experimental Setup

The device was worn continuously for 24 hours, during which time there was no specified protocol and all participants were encouraged to carry out their regular daily activity uninhibited.

TABLE I
PARTICIPANT DATA

Group	Gender	Age	BMI
Low-Fitness	2M; 9F	44-69 (59.64)	24-35 (28)
High-Fitness	2M; 9F	49-71 (57.25)	19-27 (23)

III. SIGNAL PROCESSING METHODS

For feature extraction, characteristic points need to be identified in the waveform. For T-amplitude and HR features these include the R- and T-peaks. The Q-peak was included as a useful landmark. Considering the context of remote monitoring in exercise rehabilitation, certain requirements and priorities were considered:

- Minimal operator intervention desirable
- Simplicity and low computational cost are prioritised over competitive accuracy rates
- Robustness against noise and artefacts

The ePatch® includes a built in lowpass filter with cut-off frequency of 40Hz, therefore removal of high-frequency noise is excluded here. Various methods have been described for overcoming baseline drift [5], which is important in determining T-amplitude. In this paper a method for local baseline detection is proposed in place of conventional baseline removal methods that can attenuate T-waves due their similarity in frequency spectrum to baseline drift.

Current methods for T-wave detection include template matching [6], derivative methods [7], wavelet transforms [8],[9] and phasor transforms [10] among others [11],[12]. Template matching involves selection of a template by a skilled operator, therefore is not suitable. Many of the other methods demonstrate impressive detection rates for T-peak (over 99%), but are obtained using the QT database [10] rather than data from a portable device.

In this paper, a simple derivative-based method for automatic T-peak detection is proposed that performs adequately without rigorous preprocessing. The algorithm requires *a priori* knowledge of approximate QRS complex location (a point within the QR region will suffice), and can therefore be reproduced in combination with any QRS detection module.

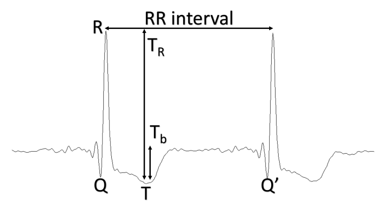

Fig. 2. Peak locations and ECG features depicted on an ePatch® signal. T_b and T_R are T-amplitude from baseline (feature T) and R-peak (feature T_R) respectively.

A. Peak Detection

The following steps are implemented to obtain peak indices in the signal. There are two inputs: (i) a binary vector, $\boldsymbol{x}$, indicating N locations of QRS complexes, and (ii) the ePatch® signal, $\boldsymbol{y}$.

1) Find R- and Q- peaks: A set of N windows ($\sim$ 0.14 seconds) are centred on the indices given in $\boldsymbol{x}$. Within these, all local maxima are located by first applying a forward difference operation, then finding transitions in polarity. The largest values within the resulting sets of local maxima are selected as R-peaks. Next, the process is repeated to find the Q-peaks, this time finding lowest local minima occurring before the R-peaks. This yields two vectors, $\boldsymbol{r}$ and $\boldsymbol{q}$, containing R and Q peak locations respectively.

2) Find T-peaks: Local regions are selected in which the T-peaks are expected. This uses the relationship between QT interval and HR as a guideline. For QT and RR intervals both in seconds, this is estimated as [13]:

$$QT = 0.4\sqrt{RR} \tag{1}$$

T-region boundary vectors, $\boldsymbol{t}_{start}$ and $\boldsymbol{t}_{stop}$, are defined as:

$$\boldsymbol{t}_{start} = \boldsymbol{q} + 4(\boldsymbol{r} - \boldsymbol{q}) \tag{2}$$

$$\boldsymbol{t}_{stop} = \boldsymbol{q} + 0.4F_s\sqrt{\Delta\boldsymbol{r}/F_s} \tag{3}$$

where $\boldsymbol{q}$ is a vector of Q-peak indices, F_s is the sampling frequency, and $(\boldsymbol{r} - \boldsymbol{q})$ and $\Delta\boldsymbol{r}$ define local QR and RR intervals (in samples) respectively. Note that these start and stop points do not necessarily correspond to actual T-wave onset and offset. Within this region, the same peak-locating technique as described for R- and Q-peak detection is implemented to find T-peaks, resulting in a vector $\boldsymbol{t}$ of T-peak locations.

B. Baseline Estimation

To overcome the effect of baseline drift, a local baseline offset is determined for each heart wave. Baseline regions are defined, then, based on their sample distributions, suitable baseline offset values are automatically selected. Baseline region boundaries are located using local peaks and intervals as:

$$\boldsymbol{b}_{start} = \boldsymbol{t} + 0.5(\boldsymbol{t} - \boldsymbol{r}) \tag{4}$$

$$\boldsymbol{b}_{stop} = \boldsymbol{q}' - 0.03F_s \tag{5}$$

where $\boldsymbol{t}-\boldsymbol{r}$ gives RT intervals and $\boldsymbol{q}'$ is a shifted version of $\boldsymbol{q}$ indicating Q-indices of the complex following the current baseline region. The margin of $0.03F_s$ in (5) excludes some of the falling slope preceding the Q-peak.

Modal values are selected as baseline offsets from the largest of 50 histogram bins in each region. This technique is more robust against the influence of outliers or presence of P- or U-waves than using mean values.

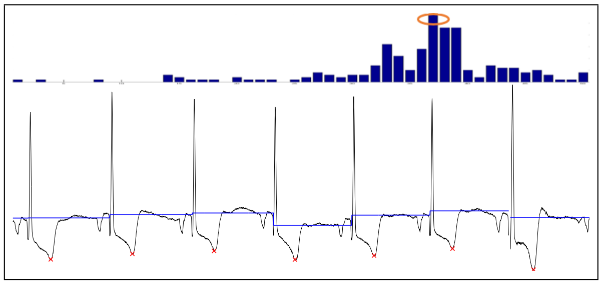

Fig. 3. Histogram of baseline region used for for baseline offset detection (top); and example showing algorithm T-peak detection (red cross) and baseline tracking (blue line) results (bottom).

C. Feature Set

Using the results of the peak and baseline detection, two T-amplitude measurements and a heart rate measurement are calculated for each ECG complex:

$$T = b - T_{peak} \tag{6}$$

$$T_R = R_{peak} - T_{peak} \tag{7}$$

$$NN = F_s \Delta \boldsymbol{r} \tag{8}$$

where b is the baseline offset, (T_{peak}) and (R_{peak}) are T-peak and R-peak values respectively, and NN is beat duration in seconds (normal-to-normal interval). T_R represents T-amplitude measured from the R-peak and is thus baseline-independent, however will be confounded with R-amplitude. Note that using (6), T-amplitude is stored as positive for comparability with data based on standard T-wave direction. From each of these series, the following four features were calculated:

- Mean (M)
- Standard deviation (SD)
- Median (Med)
- Median absolute deviation (MAD)

In the analysis, the feature abbreviations are suffixed with T or T_R for the T-amplitude features, and NN for HR features.

IV. ANALYSIS AND RESULTS

A. T-peak Detection Performance

Random samples of ePatch® data (each participant contributing equal duration) were collected to form a test set of 1,964 ECG complexes. This was analysed independently by two cardiologists and compared with the algorithm results for the same set. The two experts were unable to identify a T-peak in 5.35% and 6.92% of cases respectively. Inter-observer agreement was reported at 96.9%, and agreement between their consensus and the algorithm at 94.4%.

B. Pair-wise Testing in Grouped Feature Set

A Welch two sample t-test was used to test for differences in subject group means for the features. The results are outlined in table II where marginal and high significance are indicated by (*) and (**) respectively. For T-amplitude, *Med* and *MAD* features seem to be most significant. For HR, both mean and median are highly significant, and heart rate variability (*SDNN*) marginally significant.

TABLE II
WELCH TWO SAMPLE T-TEST

Feature	μLow	μHigh	t	df	P-value
$MeanT$	79.01	110.15	1.7916	12.819	0.096
SDT	85.65	73.55	-0.5725	18.597	0.573
$MedT$	68.74	104.93	2.0648	12.352	0.061*
$MADT$	18.38	30.61	2.1489	11.181	0.054*
$MeanT_R$	112.28	223.17	3.3576	15.157	0.004**
SDT_R	157.01	141.34	-0.4766	18.623	0.639
$MedT_R$	112.72	221.54	3.4171	15.557	0.003**
$MADT_R$	36.27	59.11	2.6956	12.493	0.019**
$MeanNN$	0.764	0.942	4.354	11.508	0.001**
$SDNN$	0.139	0.196	2.1246	13.707	0.052*
$MedNN$	0.767	0.951	4.3548	11.461	0.001**
$MADNN$	0.093	0.130	1.8966	15.148	0.077

C. Feature Correlation and Group Separation

Figure 4 shows scatter plots and Pearson correlation coefficients among a selection of features based on the pair-wise test results. These suggest negative correlation between BMI and HR features (NN), and with (T) features. The scatter plots suggest possible overlap between the groups, but feature pairs such as ($MeanNN$, $MADTR$) still offer reasonable separation.

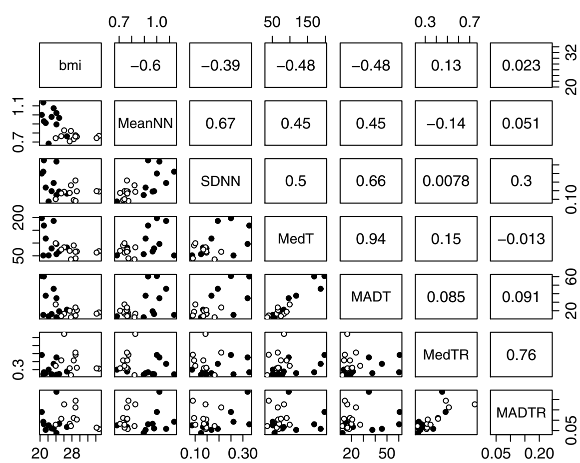

Fig. 4. Scatter plot matrix (lower triangle), where filled and empty circles indicate high- and low-fitness groups respectively. Upper triangle shows Pearson's correlation coefficients for feature pairs.

D. Data Distributions

Distributions of T, T_R and RR-interval data by group are shown in 5, from which it appears that the T-amplitude features from the high-fitness group contain at least two Gaussian subsets. Fitting a Gaussian mixture model with two components to the high-fitness T-amplitude data demonstrated which participants contributed more to each subset. Participants 1, 6 and 9 generated more T-amplitude data from the Gaussian with greater mean (Fig. 6). Interestingly, these participants also reported more training hours. Subdividing the high-fitness group by weekly training hours < 10 (*High1*) and ≥ 10 (*High2*), leads to the distributions shown in Fig. 7. Especially for T-amplitude measurement T, the low-fitness group and subset *High1* are almost indistinguishable, whereas *High2* appears quite separate.

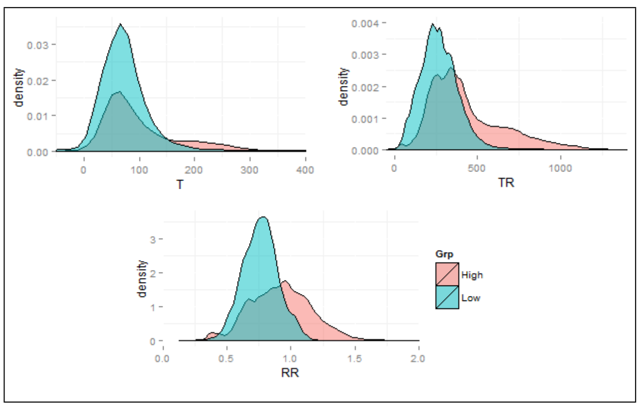

Fig. 5. Feature distributions by group: T-amplitude features measured from the baseline (top left) and from R-peak (top right); and RR interval (bottom).

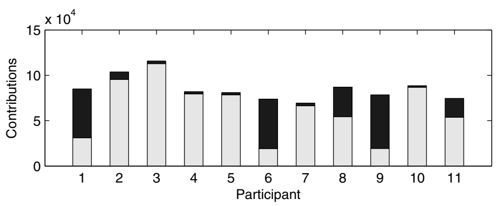

Fig. 6. T-amplitude observations of high-fitness participants, showing data assigned to Gaussian subsets 1 (grey) and 2 (black).

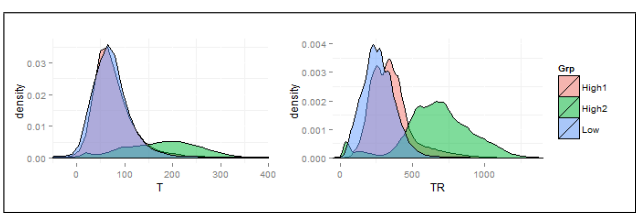

Fig. 7. Distribution of T-amplitude measured from baseline (left) and from R-peak (TR) for low-fitness and both high subsets.

V. DISCUSSION

These early findings indicate that the described setup may be beneficial for telehealth solutions in exercise rehabilitation. HR separated the groups better while T-amplitude distributions exposed within-group disparities. Participants reported that they did not notice wearing the device, and useful features were successfully extracted automatically from the data despite recording in a non-clinical environment.

A. Limitations

One limitation was possible overlap of fitness level between groups, with the only available fitness level indicators being self-reported training hours (high fitness group), lifestyle-disease risk (low-fitness group), and BMI data. Also, all factors affecting T-waves could not be measured and accounted for, thus fitness-related differences could be masked by inter-subject variation from other sources.

B. Future Work

Further research is required investigating fitness change in individuals. This approach would overcome limitations of inter-subject error, and provide insight into increment sizes to be expected in features relative to fitness increase from physical activity interventions. Additional T-wave features, and methods for selecting subsets from 24 hour recordings, could also benefit this approach.

REFERENCES

[1] Hunter, David J., and K. Srinath Reddy. Noncommunicable Diseases. NEW ENGLAND JOURNAL OF MEDICINE 369.14 (2013): 1336-1343. Web.

[2] Piotrowicz, Ewa, and Ryszard Piotrowicz. Cardiac Telerehabilitation: Current Situation and Future Challenges. European Journal of Preventive Cardiology 20.2 (2013): 12. Print.

[3] Smith, Alexandra C., David H. Saunders, and Gillian Mead. Cardiorespiratory Fitness After Stroke: a Systematic Review. INTERNATIONAL JOURNAL OF STROKE 7.6 (2012): 499-510. Web.

[4] Arbel, Yaron, Edo Y. Birati, Itzhak Shapira, Yan Topilsky, Michal Wirguin, and Jonathan Canaani. T-Wave Amplitude Is Related To Physical Fitness Status. ANNALS OF NONINVASIVE ELECTROCARDIOLOGY 17.3 (2012): 214-218. Web.

[5] Seema, M. Kaur, and B. Singh. Comparison of Different Approaches For Removal of Baseline Wander From ECG Signal. International Conference and Workshop on Emerging Trends in Technology 2011, ICWET 2011 - Conference Proceedings (2011): 1290-1294. Web.

[6] Berger, RD, EK Kasper, KL Baughman, E. Marban, H. Calkins, and GF Tomaselli. Beat-To-Beat QT Interval Variability - Novel Evidence For Repolarization Lability In Ischemic and Nonischemic Dilated Cardiomyopathy. CIRCULATION 96.5 (1997): 1557-1565. Print.

[7] Zeraatkar, Elham, Saeed Kermani, Alireza Mehridehnavi, A. Aminzadeh, E. Zeraatkar, and Hamid Sanei. Arrhythmia Detection Based On Morphological and Time-Frequency Features of T-Wave In Electrocardiogram.. Journal of Medical Signals and Sensors 1.2 (2011): 99-106. Print.

[8] Wu, Doudou, and Zhengyao Bai. An Improved Method For ECG Signal Feature Point Detection Based On Wavelet Transform. (2012): n. pag. Web.

[9] Sasikala, P., and Dr. R. S. D. Wahidabanu. Extraction of P Wave and T Wave In Electrocardiogram Using Wavelet Transform. (2011): n. pag. Print.

[10] Martinez, Arturo, Raul Alcaraz, and Jose Joaquin Rieta. Application of the Phasor Transform For Automatic Delineation of Single-Lead ECG Fiducial Points. PHYSIOLOGICAL MEASUREMENT 31.11 (2010): 1467-1485. Web.

[11] Lin, Chao, Corinne Mailhes, and Jean-Yves Tourneret. P- and T-Wave Delineation In ECG Signals Using a Bayesian Approach and a Partially Collapsed Gibbs Sampler. IEEE TRANSACTIONS ON BIOMEDICAL ENGINEERING 57.12 (2010): 2840-2849. Web.

[12] Li, Nian-Qiang, and Zheng-Sheng Wang. T-Wave Detection In Electrocardiogram Signal Based On Independent Sub-Band Function. (2009): 1-3. Web.

[13] Shuo, Yang, and Bian Desong. Automatic Detection of T-Wave End In ECG Signals. (2008): n. pag. Web.